

# Coupling between static friction force and torque for a tripod

Sylvio R. Dahmen

Instituto de Física da UFRGS, CP 15051, 90501-970 Porto Alegre RS, Brazil

Haye Hinrichsen

Fakultät für Physik und Astronomie, Universität Würzburg, D-97074 Würzburg, Germany

Andrey Lysov and Dietrich E. Wolf

Department of Physics, Universität Duisburg-Essen, D-47048 Duisburg, Germany

If a body is resting on a flat surface, the maximal static friction force before motion sets in is reduced if an external torque is also applied. The coupling between the static friction force and static friction torque is nontrivial as our studies for a tripod lying on horizontal flat surface show. In this article we report on a series of experiments we performed on a tripod and compare these with analytical and numerical solutions. It turns out that the coupling between force and torque reveals information about the microscopic properties at the onset to sliding.

PACS numbers: 46.55.+d, 81.40.Pq, 45.70.-n, 81.05.Rm

## I. INTRODUCTION

Even though most of the everyday facts about dry macroscopic friction have been known since the works of Leonardo da Vinci, Amontons, Coulomb and Euler [1], the physics of static friction, especially at the onset to sliding, is not yet fully understood. This applies in particular to bodies undergoing a simultaneous translational and rotational motion which, on account of friction, exhibit nontrivial dynamics [2, 3]. In fact, the sliding friction of a circular disk is reduced if the contact is also spinning with relative angular velocity  $\Omega_n$  (a phenomenon which plays an important role in various games such as curling or ice hockey [4, 5, 6]). It turns out that this reduction depends on the dimensionless ratio

$$\eta = \frac{v_t}{\Omega_n R}; \quad (1)$$

where  $R$  denotes the radius of the disk and  $v_t$  is the tangential relative velocity at the center of the contact area. Based on the Coulomb friction law one obtains a sliding friction force

$$F_j = \mu_d N F(\eta) \quad (2)$$

and a friction torque

$$\Gamma_j = \mu_d N R T(\eta); \quad (3)$$

where  $\mu_d$  is the dynamic friction coefficient and  $N$  is the integrated normal force acting on the contact area. Apart from the limit of pure sliding  $\eta \rightarrow 1$ , where  $F \rightarrow 1$ , the functions  $F(\eta)$  and  $T(\eta)$  depend on the pressure distribution across the contact area. Assuming uniform pressure over the area of the disk these functions have been evaluated analytically and compared with experiments [3]. An interesting phenomenon occurs in the case of sliding cylinders: due to an asymmetry in the pressure exerted on the track, which arises from the torque which tends to tip the cylinder, an analogon to the Magnus effect appears, causing the cylinder to describe curved trajectories [3, 7].

Another class of systems which has been studied extensively in a series of papers by Shegelski and coworkers is that of sliding tripods with symmetrically placed legs ( $2\pi/3$  radians apart from each other, see Fig. 1) [8]. One observes, for given initial conditions, trajectories which are serpentine (like (albeit with low lateral deflection), to curved trajectories with very large lateral deflections (curling). The translational kinetic energy may increase and decrease during a full rotation (the overall kinetic energy decreases with time). In this situation one still has a parameter analogous to  $\eta$  as in Eq. (1) but now there is a nontrivial dependence on  $\theta$  which is the angle the leg makes with the horizontal  $x$ -axis of some fixed laboratory coordinate system.

The dynamics of rotating and sliding bodies under the action of friction forces is by now fairly well understood. Not so much can be said about the statics of bodies subject to a torque and a force. Here one important question is the minimal force and torque necessary to set the body into motion and how these are coupled. That there must

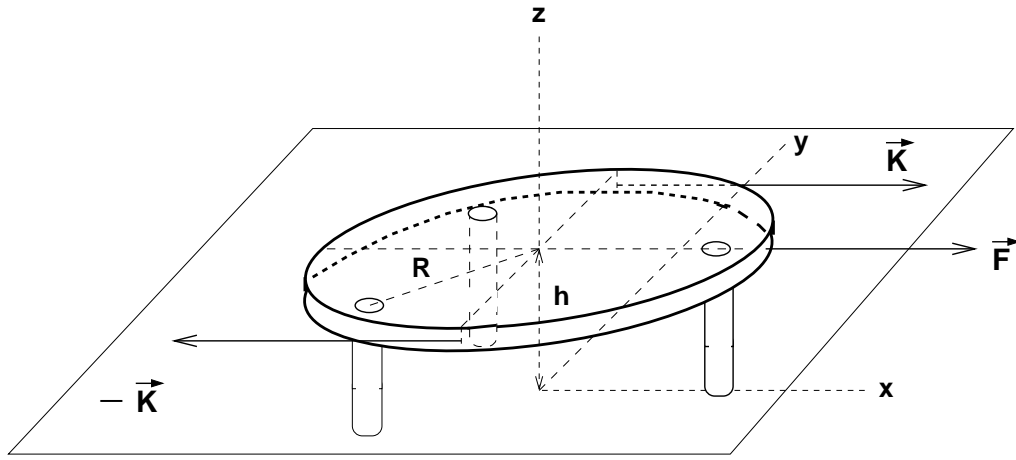


FIG. 1: The tripod experiment: bolts are evenly arranged around the perimeter and firmly attached to the disk surface. In the absence of external forces the load is equally distributed among the bolts.

be some coupling between them one knows from daily experience: if a heavy object is to be moved across the floor, it is easier to do so if one applies a torque while pushing it. Some previous analytical studies on disks showed that this is indeed the case but, contrary to the dynamical case, the static situation depends strongly on the model one uses for microscopic displacement: due to the inhomogeneity of the local displacement at each microcontact, some of them are subject to greater lateral stresses than others. One may then picture two scenarios. In the first one, a threshold is reached first at those microcontacts where the local stress is maximal. These then break irreversibly and the released stress is distributed among the remaining microcontacts. As some of these cannot sustain this increase in stress they also break, triggering an avalanche-like process where eventually all contacts detach and the disk starts to move. In the other scenario the broken microcontacts may immediately rearrange and form new contacts, redistributing the released stress over the remaining and the newly formed contact points. This microscopic stick-slip creeping continues until all contact points self-organize in such a way that they sustain on average the same stress. Therefore, by increasing the external force or torque, all microcontacts of a perfectly rigid slider reach the threshold of detachment simultaneously.

Recent experimental studies by Rubinstein and coworkers who used photoarrays to monitor the dynamics of contact points at the onset of sliding seem to favor the first scenario [9]. In their experiments a pexiglass slab was pushed in a straight line over a microscopically flat surface. Initially they observed that the microcontacts give way sequentially, propagating from the trailing edge (where the force was applied) to the front edge. The front starts propagating with about half the Rayleigh speed, accelerates and then splits up into a subsonic and an intersonic front. The time scale the contacts give way is extremely short. However, linear sliding has an intrinsic asymmetry since for an elastic body one expects the microcontacts to break where the force is applied (as the above mentioned experiments confirm) and it is not clear whether this asymmetry is in the last instance responsible for the observed phenomenon.

In this paper we study the interplay of static forces and static torques for a tripod both theoretically and experimentally. In the next section we present experimental estimates on the threshold force and torque needed to set the tripod into motion. This is followed by a theoretical section, where starting from the idea that all three feet reach the onset of sliding simultaneously, the threshold force and torque are calculated analytically. We conclude our paper with a discussion of our results and some perspectives. An appendix on an exactly solvable case is included at the end.

## II. EXPERIMENTS

In order to determine the critical line of the onset of sliding we performed a series of experiments where a pulling force and a torque were applied simultaneously to a tripod standing on a horizontal surface.

Experiments were carried out using a circular disk made of steel with radius of 86 mm. The mass was 1;123 g. The three feet, which were mechanically polished, were evenly spaced around the perimeter and placed at a distance of  $R = 80$  mm from the center of the disk, to which they were firmly attached. The tripod was provided with hooks,

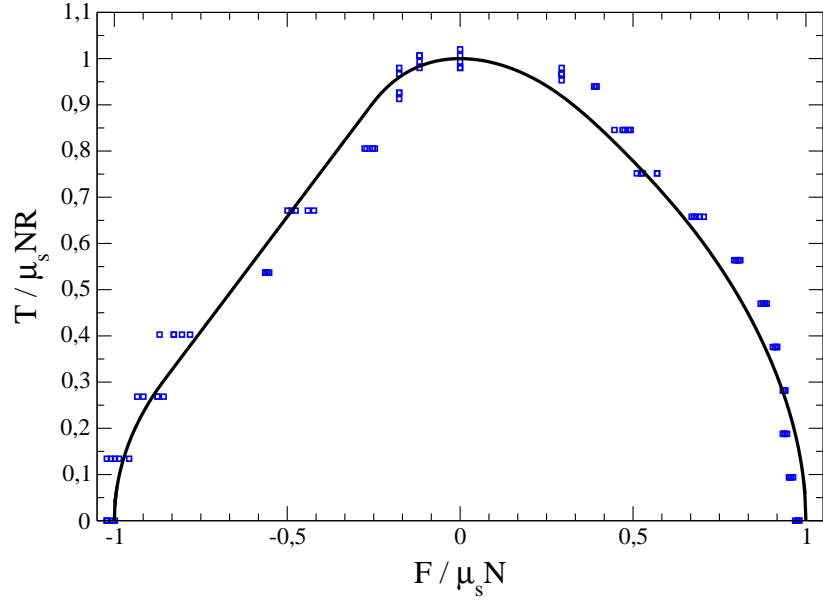


FIG. 2: Measured values of torque and force for a tripod at the onset of sliding, compared with the theoretical predictions (solid line; see text for details). Positive values of  $F$  correspond to the direction of the force as shown in Fig. 1, negative ones to the opposite direction.  $\mu_s$  is the static friction coefficient and  $N$  the weight of the tripod.

which were placed at a height of  $h = 19$  mm above the track (see Fig. 1). To measure torques and forces the tripod was placed on a fixed and microscopically flat horizontal surface. Force meters were then attached to the hooks.

Once the tripod was on the surface a torque  $T$  (as indicated in Fig. 1 by the force pair  $K$  and  $-K$ ) was applied. The disk was slowly pulled with force  $F$  until it started moving. The force meters were set to register the maximum applied pulling force  $F_c$ . For each fixed value of the torque a set of readings for the maximal force was made. The experiments were repeated several times under similar temperature and humidity conditions. We note that for very small pulling forces (large applied torques), the procedure was inverted: we fixed the force and varied the torque. This is necessary since around the region where slide sets the range of the torque values becomes extremely narrow and as it turned out, it was extremely difficult to fix the torque without displacing the disk. Steel and plastic surfaces were used and results turned out to be material independent.

Contrary to the case of a disk surface in direct contact with the track, in the tripod configuration the observed Force-Torque relationship depends not only on the microscopic scenario but also on the position of the hook points relative to the position of the bolts, i.e. on the point where the pulling force is applied. For the sake of conciseness we present in Fig. 2 the results for the case where the pulling force and torque were applied as schematically represented in Fig. 1. Negative values of  $F$  correspond to the case when the force was applied in the diametrically opposed direction.

### III. THEORETICAL PREDICTIONS

Let us consider a tripod of mass  $M$  which rests on three symmetrically arranged legs, as sketched in Fig. 3. Using a coordinate system with origin at the center of the tripod, these legs are located at unit distance  $R = 1$  at

$$\mathbf{r}_i = (\cos \varphi_i; \sin \varphi_i; 0); \quad i = 1; 2; 3 \quad (4)$$

where

$$\varphi_1 = 0; \quad \varphi_2 = 2\pi/3; \quad \varphi_3 = 4\pi/3 \quad (5)$$

The mass distribution of the tripod is symmetric, i.e., in the absence of external forces all legs carry the same weight.

As shown in Fig. 1, the tripod is subjected to external forces, namely, a linear force  $F_{\text{ext}}$  applied at the center of the disk and at height  $h$  above the track, as well as an external torque  $T_{\text{ext}}$  in form of a pair of two oppositely oriented

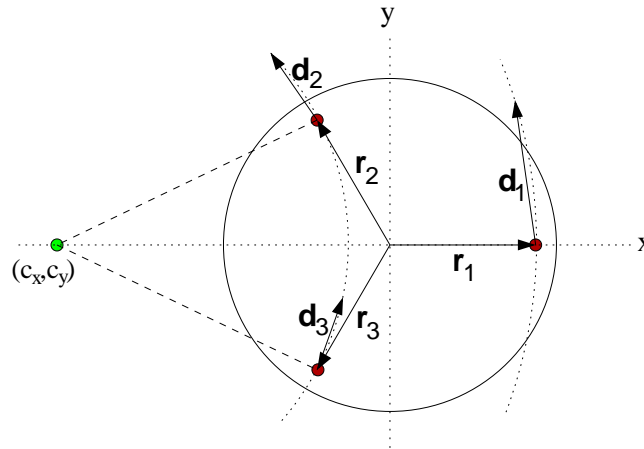


FIG. 3: Geometry for the calculation of the critical torque and force for a tripod (see text).

lateral forces  $K_x$  and  $K_y$ . We assume the tripod to be perfectly rigid. Before sliding sets in, the forces will displace and rotate the tripod infinitesimally, leading to individual microscopic displacements  $d_1; d_2; d_3$  of the contact points. Generally the displacement of the disk is a combination of a translation and a rotation with respect to the origin which (according to a well-known theorem in classical mechanics) may be viewed as a pure rotation by an angle  $\theta$  around some point

$$c = (c_x; c_y; 0) : \quad (6)$$

This point may lie inside or outside the perimeter of the tripod (see Fig. 4) and can be used to parametrize the possible displacements at the contact points

$$d_i = w \times (r_i - c) \quad i = 1::3 \quad (7)$$

where  $w = (0; 0; \theta)$ . Note that in the case of a sliding disk studied in [3], the displacements are controlled by only one parameter (see Eq. (1)) because of rotational symmetry. The same applies for the static case [10], where  $\theta$  has to be replaced by a parameter  $\theta = \frac{F_y}{R}$ . The tripod, however, is no longer rotationally symmetric and thus we have to introduce two parameters  $(c_x; c_y)$ .

As outlined in the Introduction, any theory of static friction has to make assumptions about the effective microscopic mechanism that compensates the external forces before sliding sets in. Here we use the collective breaking scenario discussed previously [10]. In this scenario it is assumed that each bolt establishes microcontacts with the track, whose number is proportional to the normal force. Each of these microcontacts can be thought of as an elastic spring. The microscopic displacement  $d_i$  deforms these springs, generating a certain restoring force in the  $xy$  plane. For small displacements these restoring forces are assumed to follow Hooke's law. However, when the restoring force at a spring reaches a certain threshold, the microcontact breaks and immediately reattaches to the surface, redistributing its stress among the other microcontacts. This leads to a microscopic stick-slip creeping motion by which the stress is continuously redistributed among the microcontacts until all of them sustain on average the same stress (even if their individual displacements  $d_i$  are different). Sliding sets in as soon as this redistributed average stress exceeds the threshold simultaneously at all contact points. This critical state at the onset to sliding defines a curve in the  $F$ - $T$  diagram. The shape of this curve is nontrivial and reveals information about the microscopic mechanism at the transition from static to sliding friction.

To determine this critical curve let us introduce the normal forces at the contact points

$$N_i = (0; 0; N_i) : \quad (8)$$

According to the collective breaking scenario described above the displacements of the contact point at the onset of sliding induce a restoring force

$$R_i = -k_s N_i e_i ; \quad (9)$$

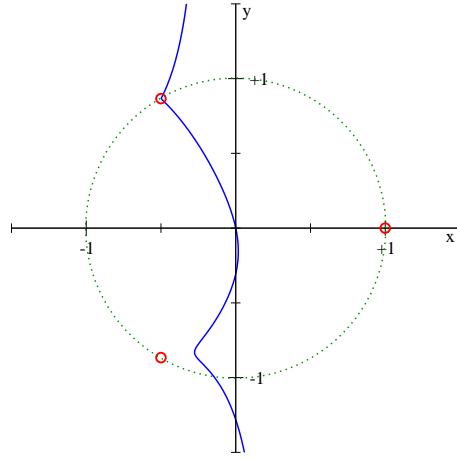


FIG. 4: Possible position of the coordinates  $c_x, c_y$  (solid line) for different values of the critical pair  $F/T$  under the condition  $F_y = 0$ , i.e., for a horizontal force. The dotted circle is the tripod's perimeter while the small circles represent the tripod's feet. The asymptotes  $y \rightarrow \pm 1$  correspond to the case of a pure translation ( $T = 0$ ), which can be interpreted as a rotation around a point at infinity. Note that for a particular pair  $(F, T)$  the vector  $c$  coincides with the position of the upper foot of the tripod. This special situation accounts for the linear segment of the  $F-T$  curve on the left-hand side of Fig. 2. The point where  $c = 0$  corresponds to the case of a pure torque ( $F = 0$ ).

where  $e_i = d_i/|d_i|$  are the unit vectors along the direction of displacement (in which  $\lambda$  cancels out) and  $\mu_s$  is the static friction coefficient. The resulting individual forces at the three legs

$$F_i = N_i + R_i \quad (10)$$

give rise to a total restoring force and a restoring torque

$$F_{\text{rest}} = \sum_{i=1}^3 F_i; \quad T_{\text{rest}} = \sum_{i=1}^3 r_i \cdot F_i \quad (11)$$

At the threshold of static friction, i.e. immediately before sliding sets in, these forces have to balance the external forces and weight of the disk, leading to the equations

$$F_{\text{rest}} + F_{\text{ext}} - M g e_z = 0 \quad (12)$$

and

$$T_{\text{rest}} + T_{\text{ext}} + h \cdot F_{\text{ext}} = 0; \quad (13)$$

where  $T_{\text{ext}} = (0; 0; \cdot)$  is the torque applied at a height  $h$  above the track and  $F_{\text{ext}} = (F_x; F_y; 0)$  is the external force applied at the point  $h = (0; 0; h)$ . Eqs. (12) and (13) form a system of six equations. Choosing a rotation center  $c = (c_x; c_y; 0)$  these equations allow one to determine the six unknowns  $N_1; N_2; N_3; F_x; F_y$ , and  $\lambda$ .

Three of the six equations, namely, the third component of Eq. (12) as well as the first and second components of Eq. (13), are linear and can be solved in order to determine the normal forces. The result reads

$$N_1 = \frac{1}{3} (M g + 2h F_x) \quad (14)$$

$$N_2 = \frac{1}{3} M g + h \left( \frac{2}{3} F_y - F_x \right) \quad (15)$$

$$N_3 = \frac{1}{3} M g - h \left( \frac{2}{3} F_y + F_x \right) \quad (16)$$

As can be seen, the external force  $F_{\text{ext}}$  applied at nonzero height  $h > 0$  leads to an additional torque and hence to different normal forces at the three bolts. As expected, for  $h = 0$  one obtains  $N_1 = N_2 = N_3 = M g/3$ .

Inserting the solution for the normal forces (14)–(16) into Eqs. (12) and (13) three nonlinear equations remain to be solved. Solving the first two components of (12) with Mathematica one obtains a highly complex non-linear expression for  $F_{\text{ext}}$  and similarly, by inserting this solution into the third component of Eq. (13), an expression for  $T$  as a function of  $c = (c_x; c_y; 0)$ . Therefore, scanning all possible values of  $c_x$  and  $c_y$  for which  $N_i \geq 0$ , one obtains the critical curve  $F = F_{\text{ext}}$  versus  $T = T_{\text{ext}}$ .

This curve is plotted in Fig. 2 as a solid line along with the experimental data, assuming that the pulling force points in horizontal direction. One may notice in this figure that there is an asymmetry in the data with respect to reactions  $F \leftrightarrow T$ , which is confirmed by our numerical solution. The reason is that the external force is applied at height  $h > 0$ , imposing an additional torque leading to different normal forces. Interestingly, this gives rise to a regime on the l.h.s. of Fig. 2, where the coordinates  $(c_x; c_y)$  coincide with the location of one of the tripod's feet, meaning that the whole tripod microscopically rotates about this pivoting point (see Fig. 4). It turns out that this happens in a noticeable range of values of  $(F; T)$  for which the values of  $c_x$  and  $c_y$  happen to be exactly under the foot. This corresponds to the region of linear dependence between force and torque. We note that for  $h = 0$  the theory would predict a symmetric curve without such a linear segment.

#### IV. CONCLUSIONS

In this paper we studied both experimentally and theoretically the coupling between static friction and torque for a tripod in dry contact with a track. Our results indicate that there is a nontrivial coupling between  $F$  and  $T$ . These results are of relevance particularly in the field of programmed motion, where one needs to program into a machine the exact forces and torques to get some task accomplished (like moving a heavy object across the floor).

Recent experiments by Rubinstein and coworkers have shown the role of propagating fronts of broken microcontacts at the transition from static to sliding friction [9]. However, due to the inhomogeneity of their experimental setup it is not clear how important a role elasticity plays. In order to assess this question one could think of repeating the photoarray experiment with a cylinder or a tripod subjected simultaneously to a torque and a pulling force. In this case each microcontacts are characterized by different displacements so that the elasticity of the body should play a minor role.

#### Acknowledgements

S.R.D. would like to thank the warm hospitality at the Institut für Physik at the University of Würzburg and at the Computational Physics Group at the University of Duisburg-Essen.

#### APPENDIX A: THE SPECIAL CASE $\alpha_1 = \pi/6; h = 0$ :

Analyzing the equations that determine the critical curve for a general angle  $\alpha_1 > 0$  between the first bolt and the x-axis in the special case of zero height  $h = 0$  we realized that the choice

$$\alpha_1 = \pi/6; \quad \alpha_2 = 5\pi/6; \quad \alpha_3 = 9\pi/6 \quad (\text{A1})$$

is special in so far as the vector pointing to the center of rotation  $c$  and the total restoring force  $F_{\text{rest}}$  are always orthogonal and aligned with the coordinate system, i.e.,

$$c_x = 0; \quad F_y = 0: \quad (\text{A2})$$

In this case the equations (12) and (13) can be simplified and solved analytically. The result (now parametrized by a single parameter  $c_y$ ) reads

$$F_x = \frac{1}{3} \left( \frac{1 - 2c_y}{1 - c_y + c_y^2} \right) \text{sgn}(1 + c_y)^A \quad (\text{A } 3)$$

$$J_j = \frac{1}{3} \left( \frac{2 - c_y}{1 - c_y + c_y^2} \right) + \text{sgn}(1 + c_y)^A : \quad (\text{A } 4)$$

Depending on the sign of  $1 + c_y$  the parameter  $c_y$  can be eliminated. In the resulting expression one has to distinguish three different cases:

$$J_j = \begin{cases} \frac{1}{2} F_x + 1 + \frac{1}{2F_x - 3F_x^2} & \text{if } 1 - F_x < \frac{1}{3}(\sqrt{3} - 1) \\ \frac{2}{3} F_x & \text{if } \frac{1}{3}(\sqrt{3} - 1) < F_x < \frac{1}{3}(\sqrt{3} + 1) \\ \frac{1}{2} F_x + 1 + \frac{1}{2F_x - 3F_x^2} & \text{if } \frac{1}{3}(\sqrt{3} + 1) < F_x \leq 1 \end{cases} \quad (\text{A } 5)$$

In the first and third case all bolts of the tripod start sliding while in the second case the tripod starts to rotate around the bolt located at  $r_3 = (0; 1; 0)$ .

- 
- [1] D. Dowson, History of Tribology, Longman, London (1979).
  - [2] S. Goyal, A. Ruina and J. Papadopoulos, Wear 143, 331 (1991).
  - [3] Z. Farkas et. al., Phys. Rev. Lett. 90, 248302-1 (2003).
  - [4] K. Vøyenli, E. Eriksen, Am. J. Phys. 53, 1149 (1985).
  - [5] T. C. Halsey, Nature 424, 1005 (2003).
  - [6] E. T. Jensen and M. R. A. Shegelski, Can. J. Phys. 82, 791 (2004).
  - [7] M. R. A. Shegelski and R. H. J. Olenstein, Can. J. Phys. 80, 141 (2002).
  - [8] M. R. A. Shegelski et al., Can. J. Phys. 82, 875 (2004).
  - [9] S. M. Rubinstein, G. Cohen, and J. Fineberg, Nature 430, 1005 (2004).
  - [10] S. R. Dahmen, Z. Farkas, H. Hinrichsen and D. E. Wolf, in preparation.